doi:10.26124/mitofit:2021-0003
Open Access

Communication

Acetyl CoA driven respiration in frozen muscle contributes to the diagnosis of mitochondrial disease

Felippe Henrique Zuccolotto-dos-Reis[1]*, PhD; Silvia Helena Andrião Escarso[1], PhD; Jackeline Souza Araujo[2], MSc; Enilza Maria Espreafico[2], PhD; Luciane Carla Alberici[3]‡, PhD; Claudia Ferreira da Rosa Sobreira[1]‡, MD, PhD.

[1] Department of Neurosciences, Division of Neurology, Ribeirão Preto Medical School, University of São Paulo, São Paulo, Brazil, Av. Bandeirantes, 3900, Monte Alegre, Ribeirão Preto, SP, 14049-900.

[2] Department of Cell and Molecular Biology, Ribeirão Preto Medical School, University of São Paulo, São Paulo, Brazil, Av. Bandeirantes, 3900, Monte Alegre, Ribeirão Preto, SP, 14049-900.

[3] Department of BioMolecular Sciences, School of Pharmaceutical Sciences of Ribeirão Preto, University of São Paulo, Ribeirão Preto, Brazil, Av. do Café s/n, Monte Alegre, Ribeirão Preto, SP, 14040-900.

‡Both authors contributed equally to the study.

*Corresponding author: felippez@alumni.usp.br Tel.: +351 926405138.

Posted Online 2021-02-19

Abstract

BACKGROUND: the procedure of freezing human biopsies is common in clinical practice as a form of storage. However, this technique disrupts mitochondrial membranes, hampering further analyses of respiratory function. To contribute to the laboratorial diagnosis of mitochondrial diseases, this study sought to develop an O_2 consumption protocol to measure the whole electron transfer system (ETS) activity in homogenates of frozen skeletal muscle biopsies.

PATIENTS AND METHODS: we enrolled 16 patients submitted to muscle biopsy in the process of routine diagnostic investigation: four with mitochondrial disease and severe mitochondrial dysfunction; seven with exercise intolerance and multiple deletions of mitochondrial DNA, presenting mild to moderate mitochondrial dysfunction; and five without mitochondrial disease, as controls. Whole homogenates of muscle fragments were prepared using grinder-type equipment.

RESULTS: Transmission electron microscopy confirmed that most mitochondria presented areas of membrane discontinuation, indicating increased permeability of mitochondrial membranes in homogenates from frozen biopsies. O_2

consumption rates in the presence acetyl-CoA lead to maximum respiratory rates sensitive to rotenone, malonate, and antimycin. This protocol of acetyl-CoA driven respiration (ACoAR), applied in whole homogenates of frozen muscle, was sensitive enough to identify ETS abnormality, even in patients with mild to moderate mitochondrial dysfunction. We demonstrated adequate repeatability of ACoAR and found a significant correlation between O_2 consumption rates and enzyme activity assays of individual ETS complexes.

CONCLUSIONS: here we present a simple, low cost and reliable procedure to measure respiratory function in whole homogenates of frozen skeletal muscle biopsies, contributing to the diagnosis of mitochondrial diseases in humans.

Keywords – frozen skeletal muscle biopsy; acetyl-CoA driven respiration (ACoAR); oxygen consumption rate; high-resolution respirometry; electron transfer system; mitochondrial diseases

1. Introduction

Mitochondria are responsible for energy production (ATP) in eukaryotes and play a central role in normal cellular function and survival. Mitochondrial diseases (MD) are a group of genetic disorders characterized by dysfunctional mitochondria. They were initially considered rare disorders, but mitochondrial dysfunction has been increasingly recognized as a cause of disease in humans [1,2]. Distinct clinical phenotypes have been associated with these disorders, encompassing both multisystem and single tissue involvement, characterizing highly variable phenotypes. Due to the lack of specific serum biomarkers, it is essential to measure mitochondrial function in affected tissues for MD diagnostic investigation. Even in the molecular era, it is not uncommon to find a mutation whose pathogenicity is not clearly defined; in this situation, functional evaluation is necessary for characterizing the underlying metabolic defect.

Enzyme assays to evaluate the activity of each complex in the mitochondrial electron transfer system (ETS) are very useful in identifying single or multiple enzyme deficiencies, while measurements of oxygen (O_2) consumption depict the entire respiratory chain activity (pathway) and the coupling between the oxidation of substrates and the phosphorylation of ADP producing ATP (oxidative phosphorylation). Both methodologies are important tools, contributing to the laboratory investigation of mitochondrial energetic dysfunction [3,4].

The ideal use of fresh tissue for the analysis of mitochondrial function is not always possible and the use of frozen samples is a reality in clinical practice. One of the advantages of frozen tissue is the possibility of storing it for future analyses. Indeed, frozen biopsies can be stable for over ten years if the samples have been frozen quickly and stored in liquid nitrogen [5]. It also allows us to perform a more extended sequence of tests, to retest samples in subsequent moments, to include stored control samples in the analysis, to analyze samples collected at locations distant from the specialized centers, and storage in biobanks for research.

While enzyme assays are routinely performed in specialized laboratories using either fresh or frozen samples, O_2 consumption requires better preservation of the tissue

[5,6,7,8,9]. Because the freezing procedure disrupts the cellular and organelle membranes, causing dissipation of mitochondrial membrane potential (ΔΨ) and other key elements for oxidative phosphorylation, O_2 consumption is traditionally performed in fresh samples, immediately after the collection of the tissue.

Previous studies successfully developed techniques for cryopreservation of tissues for later analyses of O_2 consumption, such as the one by García-Roche et al. with liver biopsies. For skeletal muscle, Kuznetsov et al. submitted the sample to dissection, permeabilization and freezing in cryopreservation solution containing DMSO and BSA. However, this is not a common procedure for sample storage at clinical laboratories and tissue biobanks. Recently, Acin-Perez et al. described protocols for measuring mitochondrial respiration in various frozen biological samples. Regarding skeletal muscle, they proposed the use of a postnuclear fraction of homogenates from frozen biopsies digested with collagenase. Respiration was evaluated using NADH as a substrate for complex I, bypassing TCA cycle.

Concomitantly, we developed an O_2 consumption protocol to analyze the electron transport pathway capacity in whole homogenates of frozen skeletal muscle biopsies from patients with mild to moderate or severe mitochondrial dysfunction and controls, using acetyl-CoA a major substrate. Due to its high demand for energy, skeletal muscle is frequently affected in mitochondrial disorders. It is also easily accessible for biopsy, which makes this tissue appropriate for the analysis of mitochondrial function in clinical practice and research.

2. Patients and methods

The ethics committee of our institution approved this study.

2.1. Patients

We selected muscle biopsies of 16 patients from the Neuromuscular Disease Clinic of our University Hospital. They were divided into three groups according to the severity of mitochondrial dysfunction in the skeletal muscle.

In the MD group, there were four patients with classical MD phenotypes, whose muscle biopsies were characterized by the presence of ragged red fibers, the hallmark of mitochondrial dysfunction in this tissue. Two of them had mitochondrial encephalomyopathy with lactic acidosis and stroke-like episodes (MELAS) caused by the mutation m.3243A>G in the gene MT-TL1, located in the mitochondrial DNA (mtDNA). The mutation was detected by next-generation sequencing of mtDNA in one patient, who harbored 91% mutant molecules, and by sequencing using the Sanger method in the second patient. The other two patients had progressive external ophthalmoplegia (PEO) due to large-scale, single mtDNA deletion (a 4977 bp deletion encompassing the nucleotides 8482 to 13460, known as the common deletion of mtDNA), detected by PCR as described by Sciacco et al. and visualized in agarose gel containing ethidium bromide. Mutation analyses in all patients were performed in DNA extracted from skeletal muscle. They were classified as presenting severe mitochondrial dysfunction because of the high

percentage of mutant mtDNA molecules or a decrease of 70% or more in the activity of at least one of the ETS complexes in relation to the median value of the controls (enzyme assays of individual ETS complexes as described below).

Seven patients with exercise intolerance as the primary symptom composed the group with mild to moderate mitochondrial dysfunction (EI group). Although a specific diagnosis was not established and muscle biopsy showed only slight, nonspecific changes, multiple deletions were found in the mtDNA extracted from skeletal muscle fragments. These multiple deletions were detected by PCR assay, with amplification of the mtDNA region between the nucleotides 7425 and 16459, using recombinant TaqDNA polymerase (Invitrogen), visualized in agarose gels containing ethidium bromide. Spectrophotometric enzyme assays of individual ETS complexes, performed as described below, demonstrated a decrease of between 30% and 70% in the activity of at least one of the ETS complexes in relation to the median value of the controls.

In the group without mitochondrial dysfunction (control group), five patients had mild proximal weakness and nonspecific findings at muscle biopsy. Multiple deletions were absent in mtDNA extracted from muscle and the activity of ETS complexes was within the normal range according to the historical controls from our laboratory (enzyme assays of individual ETS complexes as described below).

Age at muscle biopsy was similar for the EI and control groups (p=0.60 in Dunn's post hoc test); ages were also similar for the MD and control groups (p=0.24 in Dunn's post hoc test) (Table 1).

Table 1: Demographic data.

	MD group	EI group	Control group	p†
Age at biopsy (years)				
Med (min-max)	24 (8 – 42)	43 (37 – 49)	38 (32 – 48)	0.053
Gender M/F	3/1	5/2	3/2	

MD = mitochondrial disease; EI = exercise intolerance; Med = median; min = minimum; max = maximum; M = male; F = female; †Kruskal-Wallis test.

2.2. Samples

Skeletal muscle fragments from all 16 patients were collected from the biceps brachii (n=14) or quadriceps (n=2) by opened biopsy, under local anesthesia, in the course of the routine diagnostic investigation of their diseases, between the years 2000 and 2018.

Frozen samples: the skeletal muscle fragments were immediately frozen in isopentane cooled in liquid nitrogen and stored in liquid nitrogen. A fragment was taken out of its storage and thawed in ice-cold BIOPS solution (20 mM imidazole, 20 mM taurine, 50 mM KMES, 0.5 mM DTT, 10mM Ca-EGTA buffer, 6.56 mM MgCl2, 5.77 mM ATP, 15 mM phosphocreatine, pH 7.1) [14] or a TRIS-HCl buffer (0.05 M TRIS-HCl and 0.15 M KCl, pH 7.5) [15] immediately before use.

Fresh samples: biopsies from two controls were also analyzed immediately after collection. The fragments were immersed in the BIOPS solution and transported on ice to the laboratory for processing.

2.3. Preparation of whole homogenate of muscle (WHM)

Muscle biopsy fragments (45 to 100 mg) of fresh (fresh WHM) or frozen (frozen WHM) samples were weighed and a 10% weight/volume dilution was prepared in an ice-cold TRIS-HCl buffer or BIOPS solution. The fragments were homogenized with a mechanical tissue homogenizer model PowerGen 125 (Fisher Scientific, Pittsburgh, Pennsylvania, USA) turned to the maximum position (30,000 rpm). The rotor-stator generator probe used was a stainless steel probe 5 mm in diameter and 95 cm in length, which produced a shearing action on the fragment. This procedure was performed immediately before each experimental protocol. The vials containing the samples were kept in ice baths throughout the experiment.

2.4. Transmission electron microscopy (TEM)

The samples were prepared for TEM after homogenate preparation. Frozen WHM was centrifuged, the pellet was fixed for 2h at 4°C, with 2% glutaraldehyde, 2% formaldehyde, and 0.5% CaCl2 in phosphate buffer saline (NaCl 137 mM; KCl 2.7 mM; Na2HPO4 10 mM; KH2PO4 1.8 mM), and subsequently washed with 0.1 M cacodylate buffer (pH 7.4) for 1h at 4°C. The fixed components were post-fixed with 1% OsO4 for 2h at 4°C, washed with deionized water, dehydrated in a graded series of ethanol (30% to 100%), infiltrated with propylene oxide, embedded in Embed 812 resin, and left to polymerize for 72h at 60°C. Thin sections were stained with uranyl acetate and lead citrate for 10 min and examined in an electron microscope (Jeol JEM-100 CXII). We prepared two biological replicates and analyzed two grids from each. The images were processed and analyzed using the NIH-developed Image J software (National Institutes of Health, Bethesda, Maryland, USA; available at https://imagej.net). For visualization purposes, the contrast was modified using the CLAHE plugin (Stephan Saalfeld, 2010; available at https://imagej.net/Enhance_Local_Contrast_(CLAHE)), maintaining the equivalent proportions for all images.

2.5. Enzyme assays of individual ETS complexes

Spectrophotometric analyses of the activities of ETS complexes were performed in frozen WHM, considering the activities of nicotinamide adenine dinucleotide (NADH) dehydrogenase and NADH ubiquinone reductase (complex I), succinate dehydrogenase (SDH; complex II), ubiquinol cytochrome *c* reductase (complex III), cytochrome *c* oxidase (COX; complex IV), and citrate synthase (CS), as described previously, with minor modifications [15,16].

For purposes of using the same WHM for enzyme assays and O_2 consumption, the assays were performed with homogenates prepared in TRIS-HCl buffer, routinely used in these assays, and in BIOPS solution, regularly used for respirometry, for comparison.

The ETS complexes' activities were corrected according to CS, an estimated measure of mitochondrial mass. The CS activity was corrected by the wet weight of the muscle fragment and expressed as µmol of substrate/min/g of tissue.

2.6. Mitochondrial O_2 consumption protocols

Sixty µL of WHM prepared in BIOPS solution, corresponding to 6 mg of muscle, was transferred to a High-Resolution Respirometer (Oxygraph-2k, Oroboros, Innsbruck, Austria) filled with 2 mL of mitochondrial respiration buffer (MiR05) at 37ºC. The MiR05 contains: 20 mM taurine, 10 mM KH_2PO_4, 20 mM HEPES, 110 mM sucrose, 1 g/L bovine serum albumin, 0.5 mM EGTA, 3 mM $MgCl_2 \cdot H_2O$, and 60 mM K-lactobionate, pH 7.1 [14]. Electrodes were calibrated in MiR05, with a calculated saturated oxygen concentration of 185 nm/mL at 95.5 kPa barometric pressure [17]. As the samples were permeabilized by fragmentation (homogenized), chemical permeabilization techniques, such as saponin or digitonin, were not employed. Substrate and inhibitor titration protocols were carried out in duplicates. Acetyl-CoA was obtained from Sigma (catalog number A2181). The data were acquired and O_2 consumption rates were calculated using the DatLab 4 software. O_2 consumption rates were corrected by wet weight of tissue, expressed as pmol/sec/mg wet weight, or by the activity of CS. The rates of O_2 consumption in the Residual state were subtracted from the rates of the Basal and Energized states.

2.7. Statistical analysis

Numerical data were presented as median, minimum, and maximum values. Groups were compared using the non-parametric test of Kruskal-Wallis with Dunn's post hoc test. For comparison of enzyme assays performed in Tris-HCl versus BIOPS, we used the Wilcoxon test.

Correlation between enzyme assays and O_2 consumption was calculated using Spearman's correlation coefficient. The magnitude of correlation was established as proposed by Ajzen: ≤ 0.20 very low, 0.21-0.40 low, 0.41-0.60 moderate, 0.61-0.80 high, and 0.81-1.0 too high.

Repeatability of O_2 consumption measures was analyzed by the intraclass correlation coefficient (ICC) for absolute agreement, using the two-way mixed-effects model for single measures. ICC was calculated in duplicate measurements on samples from nine patients (four from the MD group, two from the EI group and three from the control group). The strength of agreement was interpreted as follows: <0.5 poor, 0.5 to 0.75 moderate, 0.75 to 0.9 good, and >0.9 excellent [19,20]. Measures 1 and 2 from those patients were also compared using the Wilcoxon test to rule out biases related to the sequence of measurement.

The significance level was set at $p < 0.05$.

The program used for the statistical analysis was the Statistical Package for the Social Sciences (SPSS) (IBM SPSS software) version 17.0. The graphs were constructed using GraphPad Prism version 5.01.

3. Results

3.1. Set-up of the O_2 consumption protocol for frozen samples

The set-up of the protocol for O_2 consumption in frozen muscle was performed using skeletal muscle biopsies of two patients from the control group. Four independent experiments were performed. Frozen and fresh muscle fragments (45 to 100 mg) from the same patient (for comparison) were homogenized (by fragmentation), generating frozen and fresh WHM, respectively.

Figure 1A shows the O_2 consumption pattern of frozen WHM submitted to routinely used respiratory protocols for fresh homogenates [17]. The respiratory rate in the frozen WHM was not changed after the addition of exogenous substrates (pyruvate and malate), ADP, oligomycin (ATP synthase inhibitor), or the ETS inhibitors rotenone and KCN, indicating a complete respiratory impairment, probably related to a disruption in mitochondrial inner membrane integrity and depolarization. A similar result was observed in the presence of cytochrome *c* (cytochrome *c* test [21], data not shown). Then, in these frozen WHM, we checked the inner membrane permeability to acetyl-CoA (Figure 1B). In the presence of cytochrome *c* and NAD^+ (to avoid the lack of these molecules due to membrane disruption) and malate (which we named Basal state), the respiratory rate was increased after the addition of acetyl-CoA (Energized state) indicating an acetyl-CoA driven respiration (ACoAR). At this state, the addition of ADP had no effect (data not shown). This condition can be considered the maximum respiratory rate because inner membrane disruption leads to H^+ return to the matrix (uncoupling), decreasing the electrochemical backpressure on the ETS proton pumps and stimulating the respiration at a maximal level flow of the ETS system. The ACoAR was sensitive to the sequential additions of the ETS inhibitors rotenone (complex I), malonate (complex II), and antimycin A (complex III), reaching an O_2 consumption rate not related to mitochondrial respiration (Residual state). After complex I inhibition, an evident inhibitory effect of malonate was observed, indicating that the TCA cycle is feeding complex II with succinate. The same protocol was applied to fresh WHM from the same patient (Figure 1C). No increment in O_2 consumption was observed after the addition of acetyl-CoA, demonstrating the known very low permeability of the mitochondrial inner membrane to high molecular mass and polar molecules. In addition, fresh WHM were tested to respiratory substrates (malate and pyruvate), ADP, and cytochrome *c*, which together led to the Energized state (Figure 1D). This state was also sensitive to ETS inhibitors; however, the inhibitory effect of malonate was less evident than that observed in the frozen WHM. This effect probably occurs because pyruvate reduces one additional NAD^+ at the pyruvate dehydrogenase complex, generating a higher proportion of NADH:FADH2 (4:1) compared to acetyl-CoA (3:1), thereby supplying more electrons to complex I. Note that the O_2 consumption rates in Energized states of fresh (Figure 1D) and frozen (Figure 1B) WHM are very similar (~ 7 pmol O_2/(s*mg)), demonstrating that the protocol developed in this study for whole homogenates of frozen samples allows for the reaching of the same maximal respiratory rates found in whole homogenates of fresh samples.

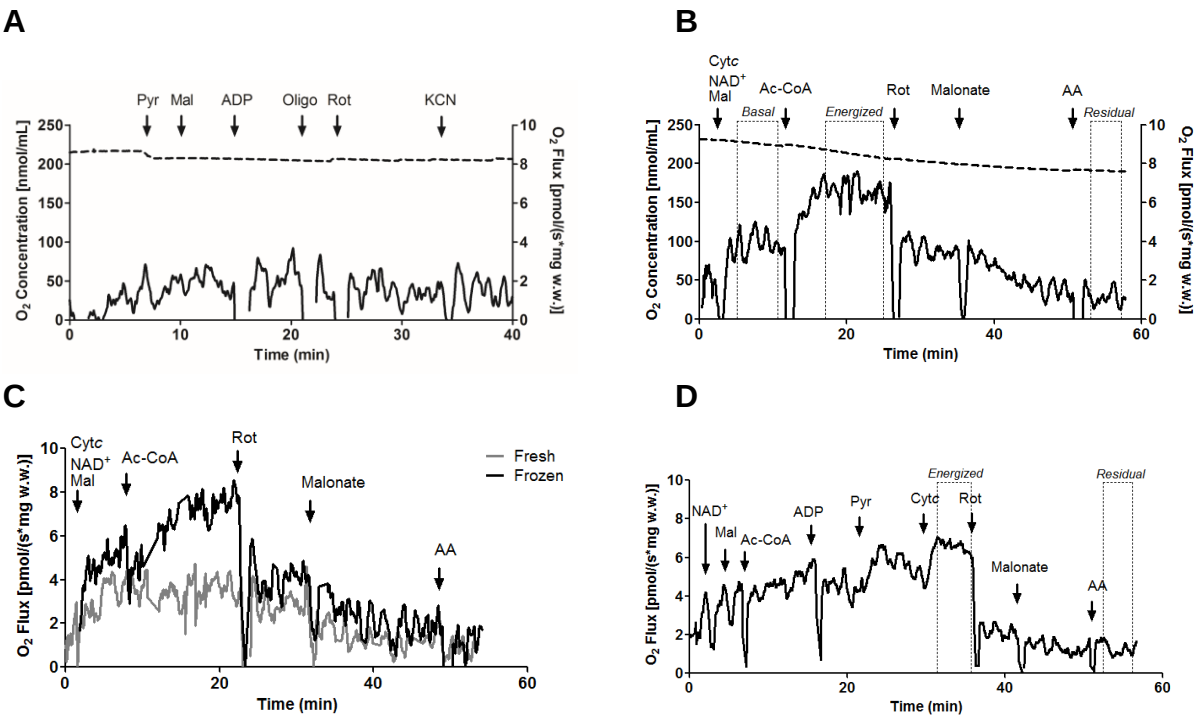

Figure 1. Oxygen consumption in frozen and fresh WHM from the control group. The samples were homogenized in the BIOPS medium, and O_2 consumption was evaluated in the MIR05 medium as described in the materials and methods section. Representative trace of O_2 consumption by frozen WHM (A and B). The upper line indicates the O_2 concentration in the oxygraphy chamber (nmol/mL) and the lower line indicates the rates of O_2 consumption (pmol/sec/mg wet weight (w.w.) of tissue). Representative trace of O_2 consumption rates by frozen and fresh WHM (C) or fresh WHM (D), n = 2. The arrows indicate the addition of pyruvate (Pyr), malate (Mal, 2 mM), ADP, oligomycin (oligo), rotenone (Rot, 1 µM), KCN, cytochrome *c* (cyt*c*, 10 µM), β-NAD (NAD^+, 100 µM), acetyl-CoA (Ac-CoA, 150 µM), malonate (5 mM), or antimycin A (AA, 2.5 mM). States were determined after the addition of cytochrome c (cytc), NAD^+ and malate (Basal), acetyl-CoA (Ac-CoA) (Energized) representing the acetyl-CoA driven respiration (ACoAR), and antimycin A (AA) (Residual).

To demonstrate the rupture of mitochondrial membranes after the freezing process and reinforce the idea of acetyl-CoA permeability in the inner membrane, we performed transmission electron microscopy (TEM) (Figure 2). For this, frozen muscle biopsies of two patients (one from the control group and one from the MD group) were selected. Although part of the mitochondrial structure was preserved in some organelles (head arrows), most mitochondria presented clearly identified areas of membrane discontinuation (arrows) in homogenates of controls (A, A', and A") or MD patients (B, B', and B"). These fissures can increase the permeability of mitochondrial membranes, thereby blending the matrix and extramitochondrial environment, suggesting that added

acetyl-CoA can easily participate in the generation of reduction power by the TCA cycle (NADH and FADH2) to supply the respiratory chain.

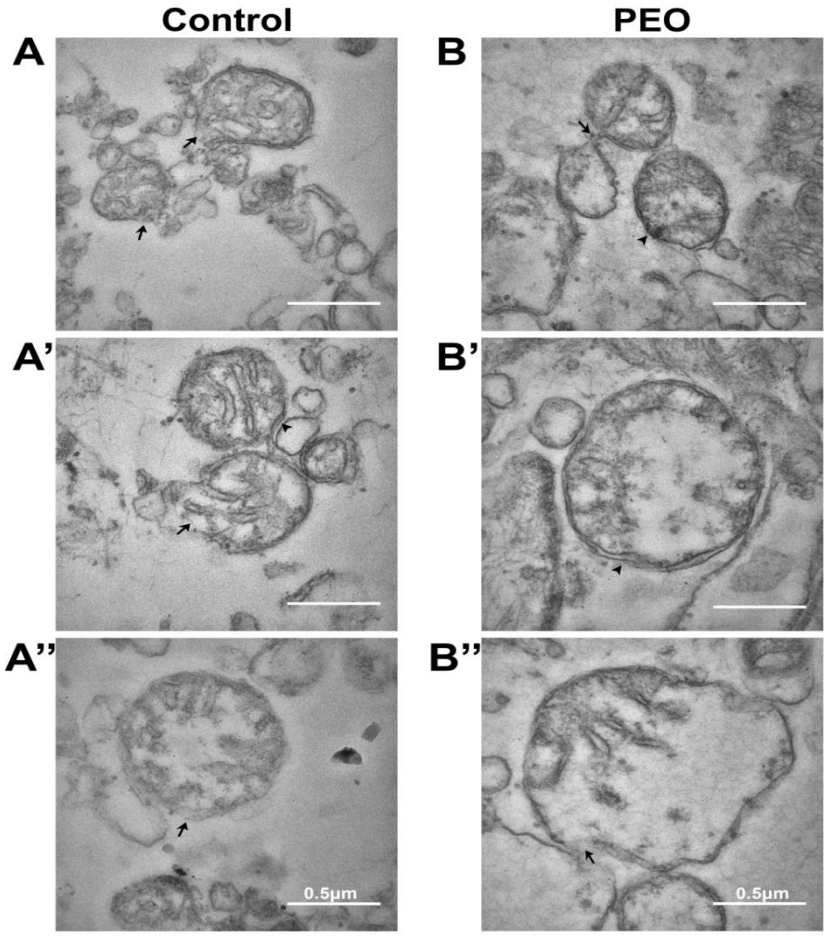

Figure 2. Mitochondrial ultrastructure in frozen WHM. Representative micrographs showing the mitochondrial ultrastructure in homogenates in two patients: one from the control (A) group and one from the MD (B) group. The arrows indicate the ruptured double membranes of the mitochondria, while the arrow heads indicate mitochondria with more preserved membranes. Scale bar = 0.5 µm with increase of 100,000x.

3.2. Comparison between control, EI, and MD groups

Using the protocol for frozen WHM preparation described above, we measured the O_2 consumption in samples obtained from patients with different degrees of mitochondrial dysfunction and in controls (Figure 3). As patients with mitochondrial dysfunction may present a compensatory increase in mitochondrial mass [22], O_2 consumption rates were normalized by the CS activity (a usual marker of mitochondrial content) of each sample. The results show that WHM of the EI and MD groups presented reduced respiratory rates in both Basal state and ACoAR compared to controls,

indicating the accuracy of our protocol, which was able to identify even the mild to moderate levels of mitochondrial dysfunction.

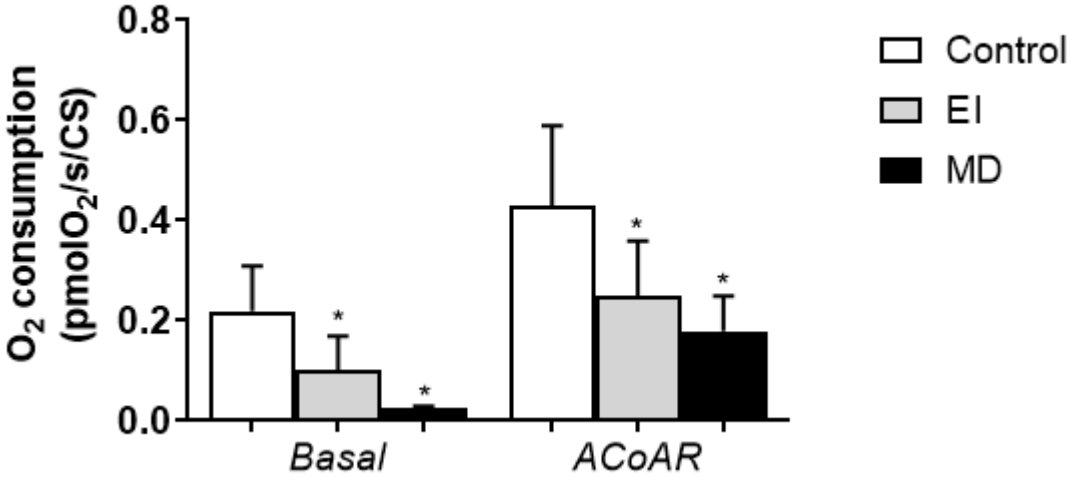

Figure 3. Oxygen consumption rates in frozen WHM from control (n=5), EI (n=7) and MD (n=4) patients of similar ages. Respiration rates in the presence of acetyl-CoA (ACoAR) or not (Basal state), normalized to citrate synthase (CS) activity. The rates of O_2 consumption in the Residual state were subtracted from Basal and Energized (ACoAR) rates. Bar graphs show the median and variances. Data from those patients whose experiments were performed as duplicates were included as the average of the two measurements. The Kruskal-Wallis test determined that rates of O_2 consumption were different between groups (p=0.004 for both the Basal state and the ACoAR). The statistical differences in relation to the controls are indicated in the chart by *, with p = 0.04 between control and MD groups, p = 0.01 between control and EI groups and p = 0.26 and 0.39 (respectively for Basal state and ACoAR) between MD and EI groups according to the Dunn's post hoc test.

3.3. Correlation to enzyme assays of individual ETS complexes

To better characterize the accuracy of the ACoAR protocol for frozen samples of control, EI, and MD groups, we correlated respiration results to the enzyme activity of individual ETS complexes. As in O_2 consumption rates, ETS complex activities were normalized by CS activity. Therefore, we initially compared the results of enzyme activity performed in WHM prepared in BIOPS solution to WHM made in TRIS-HCl, the buffer routinely used in those assays. Except for CIV, all other enzyme complexes and CS showed similar results in both solutions (CI p=0.76; CII p=0.34; CIII p=0.09; CS p=0.42). CIV activity was higher in TRIS-HCl buffer (p=0.004); however, the values obtained using BIOPS solution in the control group were also within the normal range expected for the assay.

The results of enzyme assays performed in the BIOPS medium are shown in Table 2. The MD group presented a significant decrease in the activities of all ETS complexes. The patients with EI, however, as a group, did not differ from the controls.

Table 2. Enzyme assays of ETS and citrate synthase.

	MD group	EI group	Control group	p†
	Med (min – max)	Med (min – max)	Med (min – max)	
Citrate synthase	20.7 (13.7 – 49.7)	15.6 (10.8 – 20.5)	12.5 (10.6 – 15.6)	0.09
CI	0.13* (0.01 – 0.22)	0.33# (0.15 – 0.37)	0.45 (0.29 – 0.55)	0.006
CII	0.15* (0.11 – 0.20)	0.23# (0.20 – 0.40)	0.38 (0.31 – 0.45)	0.007
CIII	0.23* (0.21 – 0.33)	0.25 (0.20 – 0.54)	0.48 (0.41 – 0.52)	0.03
CIV	0.26* (0.21 – 0.36)	0.37 (0.26 – 0.76)	0.75 (0.57 – 0.77)	0.01

ETS=electron transfer system; MD = mitochondrial disease; EI = exercise intolerance; Med = median; min = minimum; max = maximum; citrate synthase values are expressed in µmol/min/g wet tissue; activities of complexes I to IV (CI to CIV) are corrected to citrate synthase activity; group MD n=4; group EI n=7 (except in CII, where n=6) and control group n=5. †Kruskal-Wallis test. * Indicates a significant difference in relation to the control group in the Dunn's post hoc test. # Indicates a significant difference in relation to the MD group in the Dunn's post hoc test. The fragments were homogenized in BIOPS solution and evaluated in specific media for each reaction, with compositions and assays described in the methods.

The correlation between O_2 consumption rates in the Energized state (ACoAR) and the activities of individual ETS enzyme complexes were moderate and positive, indicating that both procedures measure related phenomena (Table 3).

Table 3. Correlation between assays of O_2 consumption at the Energized state ACoAR and enzyme assays of individual ETS complexes.

		CI (n=16)	CII (n=15)	CIII (n=16)	CIV (n=16)
O_2 consumption	r	0.597	0.721	0.688	0.678
	p	0.015	0.002	0.003	0.004

ACoAR = acetyl-CoA driven respiration; ETS = electron transfer system; CI to CIV (complex I to IV); r = Spearman's correlation coefficient; n = number of individuals

3.4. Repeatability

The method of measuring O_2 consumption rates proposed herein, using frozen WHM, showed adequate repeatability. The strength of agreement for the Basal state O_2 consumption rate was too variable, ranging from poor to excellent according to the 95% confidence interval (ICC=0.83, 95% confidence interval 0.30 – 0.96). However, measurements of O_2 consumption rates at the Energized state (ACoAR) were highly

reliable, with strengths of agreement classified as good to excellent (ICC=0.95, 95% confidence interval 0.81 – 0.99).

The Wilcoxon test indicated similarity between the groups of measures 1 and 2 at both states (p=0.73 for O_2 consumption rates at the Energized state; p=0.31 for O_2 consumption rates at the Basal state), ruling out a bias related to the order of measurement.

4. Discussion

The possibility of studying mitochondrial respiratory function of skeletal muscle using frozen biopsy fragments contributes to the laboratory assessment of patients with mitochondrial disease. Enzyme assays of individual ETS complexes are routinely analyzed in frozen samples in some specialized laboratories. However, mild decreases in the activity of ETS complexes may not be identified by the assays, which may disclose normal results in a relatively high proportion of patients with abnormal mitochondrial function [23]. In fact, as a group, our patients with milder mitochondrial dysfunction (EI group) did not differ from the control group regarding the activity of ETS complexes and CS, although individually they presented a mild or moderate decrease in the activity of at least one of the ETS complexes in relation to the median value of the controls. Moreover, mild to moderate deficiencies identified in ETS enzyme assays should be confirmed by additional methods to be validated [24,25]. To meet those needs, we developed a method for measuring O_2 consumption using high-resolution respirometry, so that it could be applied in frozen skeletal muscle biopsies.

The first challenge was to define how to process frozen muscle samples before measuring O_2 consumption.

Mitochondrial isolation methods usually retrieve only part of the mitochondrial content from muscle and raise concerns regarding the selection of mitochondria [26]; moreover, these procedures were designed for application to fresh tissues. On the other hand, fiber permeabilization is a model already recognized for O_2 consumption studies, which preserves the mitochondrial architecture, its three-dimensional network, and the interaction with cellular components essential for mitochondrial function [26,27]. However, this technique can not be applied in frozen samples, because before freezing, skeletal muscle needs to be dissected, permeabilized and stored in cryopreservation solution containing 30% DMSO and 10 mg/ml BSA [11].

Homogenates of fresh tissue have already been used for respirometry. The main challenges of this technique were the damage to the structure of the CI and the outer mitochondrial membrane [28]. Ziak et al. have demonstrated that the homogenization technique causes only minor damage to the outer mitochondrial membrane and the respiratory complexes. In their study, reliable results could be achieved in homogenates obtained from muscle biopsy samples, provided that the respirometry was performed soon after the homogenization of the samples. Starting from frozen biopsies, respiratory

activity in homogenates was successfully measured in a postnuclear fraction, using NADH as a substrate for complex I, given the damage of the inner membrane from freeze–thaw. However, in this protocol TCA cycle was considered impaired [12].

Based on the above points, we chose to use WHM prepared with grinder-type equipment with a rotor-stator generator probe, which homogenizes the tissue through fragmentation, instead of chemical/enzymatic permeabilization, to avoid interference of these molecules on respiratory function.

Analyses of the mitochondrial ultrastructure of these frozen WHM showed that the membranes contain fissures, allowing for exchanges of ions, substrates, and perhaps enzymes. This explains the stimulatory effect of acetyl-CoA on respiration in homogenates from frozen WHM. Such a response was not observed in homogenates from fresh WHM, indicating that the mitochondrial membrane disruption was derived from the freeze-thaw procedure, with little influence of homogenization. These data agree with the study by Birch-Machin et al., who evaluated various membrane rupture methods and concluded that mitochondrial freeze-thaw is a crucial procedure for quantifying the activity of ETS enzymes and CS.

Therefore, our protocol involves the use of acetyl-CoA and malate as substrates for respiration measurements (ACoAR). They were satisfactory substrates set for the full energization of the ETS and the reproducibility of the procedure in frozen WHM. In the presence of sufficient NAD^+, malate and acetyl-CoA can feed the TCA cycle, which metabolizes acetyl-CoA, generating reduced coenzymes (NADH and FADH2) in four of eight steps. NADH and FADH2 donate their protons and electrons to the ETS enzyme complexes CI and CII, respectively, in oxido-reduction reactions. Arriving at the CIV, the electrons reduce molecular O_2 to H_2O, thus consuming the O_2.

Another essential step in the analysis was the correction of the O_2 consumption rates according to the mitochondrial mass, derived from the quantification of CS activity in the same homogenate. The respiration traces, when normalized by wet weight, did not present a significant difference between the groups because the mitochondrial proliferation observed in the patients partially compensates for the deficiency of O_2 consumption per mitochondrion. However, our ACoAR protocol was able to differentiate individuals with a mitochondrial disease from controls when we corrected O_2 consumption rates by the CS activity of each sample. The ACoAR protocol for frozen WHM was also capable of differentiating the group of patients with mild to moderate mitochondrial dysfunction (EI group) from controls, which was not achieved by enzyme assays of individual ETS complexes. Because O_2 consumption depicts the entire respiratory chain pathway, the summation of smaller changes in individual complexes may favor the identification of milder functional abnormalities. The finding of a significant correlation between the results of individual ETS enzyme assays and O_2 consumption rates indicates that the protocol developed here for frozen samples is a valid procedure for measuring respiratory chain function.

In conclusion, the protocol developed here for sample preparation and O_2 consumption measurement of frozen skeletal muscle biopsies was shown to be a valid and reliable method for investigating mitochondrial respiratory function, which should include a combination of clinical and laboratory analyses to increase the diagnostic power.

Acknowledgements

This study was financed by the Fundação de Amparo à Pesquisa do Estado de São Paulo (FAPESP) [grant numbers 2017/04372-0, 2016/23509-4]. This study was financed in part by the Coordenação de Aperfeiçoamento de Pessoal de Nível Superior - Brasil (CAPES) - Finance Code 001 (Felippe H. Zuccolotto-dos-Reis received a PhD scholarship). Jackeline S. Araujo has a FAPESP fellowship [grant number 2016/10862-8]. Luciane C. Alberici has a CNPq Research Fellowship. Claudia F.R. Sobreira and Silvia H.A. Escarso are part of the Center for Integrative Systems Biology (CISBi) - NAP/University of São Paulo. The authors are grateful to Geraldo Cássio dos Reis for assistance in the statistical analyses, as well as Thaísa Gomes Tognati Ikuma for technical support. The authors acknowledge the use of the core facility of Transmission electron microscopy from Laboratório Multiusuário de Microscopia Eletrônica (LMME) of Ribeirão Preto Medical School, University of São Paulo.

Author contributions

Felippe H. Zuccolotto-dos-Reis contributed to the conception or design of the work, acquisition, analyses or interpretation of data, writing the original draft, reviewing and editing. Silvia H. A. Escarso contributed to acquisition, analyses or interpretation of data. Jackeline S. Araújo contributed to acquisition of data. Enilza M. Espreafico contributed to analyses or interpretation of data. Luciane C. Alberici and Cláudia F. R. Sobreira contributed to the conception or design of the work, analyses and interpretation of data, writing, reviewing and critically revising the manuscript. All gave final approval and agreed to be accountable for all aspects of work ensuring integrity and accuracy.

Conflicts of interest

The authors declare that there is no conflict of interests or financial disclosures.

Abbreviations

AA, antimycin A; ACoAR, acetyl-CoA driven respiration; ADP, adenosine diphosphate; ATP, adenosine triphosphate; BSA, bovine serum albumin; CI, CII, CIII and CIV, complexes I, II, III and IV; COX, cytochrome *c* oxidase; CPEO, chronic progressive external ophthalmoplegia; CS, citrate synthase; DMSO, dimethyl sulfoxide; DNA, deoxyribonucleic acid; DTT, dithiothreitol; EGTA, ethylene glycol tetraacetic acid; EI, exercise intolerance; ETS, electron transfer system; $FADH_2$, flavin adenine dinucleotide (reduced state); HEPES, 4-(2-hydroxyethyl)-1-piperazineethanesulfonic acid; ICC, intraclass correlation coefficient; KMES, 2-(N-Morpholino)ethanesulfonic acid potassium salt; MD, mitochondrial disease; MELAS, mitochondrial encephalomyopathy with lactic acidosis and stroke-like episodes; mtDNA, mitochondrial DNA; NADH, nicotinamide adenine dinucleotide (reduced state); NAD^+, nicotinamide adenine dinucleotide (oxidized state); PCR, polymerase chain reaction; SDH, succinate dehydrogenase; TCA, tricarboxylic acid cycle; TEM, transmission electron microscopy; TRIS-HCl, 2-Amino-2-(hydroxymethyl)-1,3-propanediol hydrochloride; WHM, whole homogenate of muscle.

504 ## References

505 1. Gorman GS, Schaefer AM, NG Y, et al. Prevalence of nuclear and mitochondrial DNA mutations
506 related to adult mitochondrial disease. Ann Neurol. 2015;77(5):753-759.
507 2. Gorman GS, Chinnery PF, Dimauro S, et al. Mitochondrial diseases. Nature Reviews Disease
508 Primers 2016;2: article n. 16080.
509 3. Kirby DM, Thorburn DR, Turnbull DM, Taylor RW. Biochemical Assays of Respiratory Chain
510 Complex Activity. Methods in Cell Biology 2007;80:93-119.
511 4. Gnaiger E. Capacity of oxidative phosphorylation of human skeletal muscle. New perspectives
512 of mitochondrial physiology. The International Journal of Biochemistry & Cell Biology
513 2009;41:1837-1845.
514 5. Thorburn DR, Chow CW, Kirby DM. Respiratory chain enzyme analysis in muscle and liver.
515 Mitochondrion 2004;4:363-375.
516 6. Gellerich FN, Mayr JA, Reuter S, Sperl W, Zierz S. The problem of interlab variation in methods
517 for mitochondrial disease diagnosis: enzymatic measurement of respiratory chain complexes.
518 Mitochondrion 2004;4:427–439.
519 7. Medja F, Allouche S, Frachon P, et al. Development and implementation of standardized
520 respiratory chain spectrophotometric assays for clinical diagnosis. Mitochondrion
521 2009;9:331-339.
522 8. Rodenburg RJ T. Biochemical diagnosis of mitochondrial disorders. JIMD 2011;34(2):283-292.
523 9. Spinazzi M, Casarin A, Pertegato V, Salviati L, Angelini C. Assessment of mitochondrial
524 respiratory chain enzymatic activities on tissues and cultured cells. Nature Protocol
525 2012;7:1235-1246.
526 10. Garcia-Roche M, Casal A, Carriquiry M, Radi F, Quijano C, Cassina A. Respiratory analysis of
527 coupled mitochondria in cryopreserved liver biopsy. Redox Biology 2018:17:207-212.
528 11. Kuznetsov AV, Kunz WS, Saks V, et al. Cryopreservation of mitochondria and mitochondrial
529 function in cardiac and skeletal muscle fibers. Analytical Biochemistry 2003;319:296-303.
530 12. Acin-Perez R, Benado IY, Petcherski A, et al. A novel approach to measure mitochondrial
531 respiration in frozen biological samples. The EMBO Journal 2020;39:104073.
532 13. Sciacco M, Bonilla E, Schon EA, Dimauro S, Moraes CT. Distribution of wild-type and common
533 deletion forms of mtDNA in normal and respiration-deficient muscle fibers from patients with
534 mitochondrial myopathy. Hum Mol Genet. 1994;3:13-19. Erratum in: Hum Mol Genet
535 1994;3(4):687.
536 14. Larsen S, Wright-Paradis C, Gnaiger E, Helge JW, Boushel R. Cryopreservation of human
537 skeletal muscle impairs mitochondrial function. CryoLetters 2012;33:169-175
538 15. Dimauro S, Servidei S, Zeviani M, et al. Cytochrome c oxidase deficiency in Leigh syndrome.
539 Ann Neurol 1987;22:498-506
540 16. Birch-Machin MA, Briggs HL, Saborido AA, Bindoff LA, Turnbull DM. An evaluation of the
541 measurement of the activities of complexes I-IV in the respiratory chain of human skeletal
542 muscle mitochondria. Biochemical Medicine and Metabolic Biology 1994;51:35-42
543 17. Pesta D, Gnaiger E. High-resolution respirometry: OXPHOS protocols for human cells and
544 permeabilized fibers from small biopsies of human muscle. In: Palmeira CM, Moreno AJ. (Eds.).
545 Mitochondrial Bioenergetics: Methods and Protocols. Springer Science+Business Media; 2012.
546 25-30 p.
547 18. Ajzen I. Understanding attitudes and predicting social behavior. New Jersey: Prentice-Hall,
548 Inc., Englewood Cliffs; 1998. 97-99 p.
549 19. Shrout PE, Fleiss JL. Intraclass correlations: uses in assessing rater reliability. Psychol Bull
550 1979;86:420-428.

20. Koo TK, Li MY. A guideline of selecting and reporting Intraclass Correlation Coefficients for Reliability Research. J Chiropractic Med 2016;15:155-163.
21. Lanza IR, Nair KS. Functional assessment of isolated mitochondria in vitro. Methods Enzymol 2009;457:349-372.
22. Sobreira C, Hirano M, Shanske S, et al. Mitochondrial encephalomyopathy with coenzyme Q10 deficiency. Neurology 1997;48:1238-1243.
23. Thorburn DR, Smeitink J. Diagnosis of mitochondrial disorders: clinical and biochemical approach. J Inherit Metab Dis 2001;24(2):312-316.
24. Bernier FP, Boneh A, Dennett X, Chow CW, Cleary MA, Thorburn DR. Diagnostic criteria for respiratory chain disorders in adults and children. Neurology 2002;59:1406-1411.
25. Thorburn DR, Sugiana C, Salemi R, et al. Biochemical and molecular diagnosis of mitochondrial respiratory chain disorders. BBA-Bioenergetics 2004b;1659(2-3):121-128.
26. Picard M, Taivassalo T, Ritchie D, et al. Mitochondrial Structure and Function Are Disrupted by Standard Isolation Methods. PLoS One 2011;6(3):e18317.
27. Kuznetsov AV, Veksler V, Gellerich FN, Saks V, Margreiter R, Kunz WS. Analysis of mitochondrial function in situ in permeabilized muscle fibers, tissues and cells. Nature Protocols 2008;3:965–976.
28. Larsen S, Kraunøe R, Gram M, Gnaiger E, Helge JW, Dela F. The best approach: Homogenization or manual permeabilization of human skeletal muscle fibers for respirometry? Analytical Biochemistry 2014;446:64-68.
29. Ziak J, Krajcova A, Jiroutkova K, Nemcova V, Dzupa V, Duska F. Assessing the function of mitochondria in cytosolic context in human skeletal muscle: Adopting high-resolution respirometry to homogenate of needle biopsy tissue samples. Mitochondrion 2015;21:106-112.